DOI: 10.1002/ejic.200900153

Preparation of Mesoporous Silica and Carbon Materials with Multilength-Scale Pores and Hydrogen Sorption Application

Tae-Hwan Kwon,[a] Suhyun Jung,[b] Hee-Jin Kim,[c] Seongsoon Park,[b] Sung-Jin Kim,[c] and Seong Huh*[a]

Keywords: Mesoporous materials / Silica / Carbon / Hydrogen storage / Nanostructures

A facile method was developed for the preparation of bimodal mesoporous siliceous materials with nanostructured pores in which a cationic organic template, *n*-hexadecyltrimethylammonium hydroxide, was employed as a base catalyst as well as a mesopore structure-directing agent during the slow condensation of tetraethoxysilane. It was possible to alter the pore orientations of smaller pores by adding neutral auxiliary templates such as Brij76 and P123. A series of bimodal mesoporous carbons was also obtained from the bimodal mesoporous silica materials through a nanocasting process. The resulting bimodal mesoporous carbons exhibited decent hydrogen uptake values at 77 K. The maximum hydrogen uptake was 1.33 wt.-% for the sample having the narrowest pores, while keeping a relatively large pore volume.

Introduction

Nanoporous materials with multilength-scale pores is an important class of nanomaterials in the applications of catalyst supports and adsorbents.[1] Since the first report of the mesoporous silica MCM-41 family, an enormous number of publications has described the preparation of these novel materials.[2] Meanwhile, a few attempts to prepare multilength-scale nanoporous structures by using multiple templates have been reported.[3] In these cases, however, strict preparation conditions and judicious choice of templates are prerequisites to obtain the desired materials. In addition, most of the current synthetic methods to prepare bimodal or trimodal mesoporous materials depend on the hard templating approach, which is also called either nanocasting or exotemplating. Therefore, we have been interested in finding more efficient methods to prepare these important classes of materials. Herein, we report a facile method to prepare bimodal mesoporous silica and related carbon materials. The motif of our approach is the use of cetyltrimethylammonium hydroxide (CTAOH) as a hydrolysis catalyst of tetraethoxysilane (TEOS) as well as a cationic template under very low concentration of CTAOH template. It was observed that the low concentration of the cationic template induced small micron-sized particles in the base-catalyzed mesoporous silica preparations.[4,5] Therefore, we attempted to use CTAOH instead of the conventional cetyltrimethylammonium bromide (CTABr) template. Extra base catalysts were not required during the material preparation. As a result of the low concentration of CTAOH and the absence of additional hydrolysis catalysts, the hydrolysis and condensation rates of silica precursors such as TEOS must be very slow. More importantly, the majority of the hydroxide ions are believed to reside in the Stern layer because of the strong electrostatic interaction with the CTA^+ head groups of the micelles.[5] Hence, the TEOS hydrolysis by the hydroxide ions might occur near the surface of the micelles. This kinetic control of hydrolysis and condensation of TEOS at the surface of positively charged micelles would produce small-sized silicate nanoparticles. Their aggregates further generate extra voids because of their loose interconnections as shown in Figure 1.

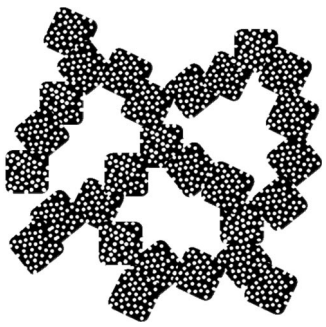

Figure 1. A drawing of the proposed bimodal pore structure.

[a] Department of Chemistry and Protein Research Center for Bio-Industry, Hankuk University of Foreign Studies,
Yongin 449-791, Korea
Fax: +82-31-330-4566
E-mail: shuh@hufs.ac.kr
[b] Department of Chemistry, Center for NanoBio Applied Technology and Institute of Basic Sciences, Sungshin Women's University,
Seoul 136-742, Korea
[c] Division of Nano Sciences and Department of Chemistry, Ewha Woman's University,
Seoul 120-750, Korea

Results and Discussion

The molar ratio of the starting materials CTAOH/H_2O/TEOS was 1.0:8030:11.6. TEOS was added into the preheated aqueous CTAOH solution at 353 K with constant stirring. The reaction mixture was further heated for 24 h. Unlike the CTAB template, the CTAOH template required a longer reaction time to get solid product because of the much slower condensation rate. The as-prepared product was retrieved by filtration and washed with a copious amount of water. The as-prepared gel was dried in an oven at 353 K overnight. The template-free material, denoted as BMS-1 (BMS = bimodal mesoporous silica), was obtained after calcination in air at 823 K. The calcined sample was fully characterized by N_2 sorption analysis at 77 K, field emission transmission electron microscopy (FETEM), high-resolution scanning electron microscopy (HRSEM), and powder X-ray diffraction (XRD). It is noteworthy to mention that the measured pH value of the CTAOH solution before the addition of TEOS under our synthetic conditions was 11.3, which indicated that the solution was sufficiently basic. Nevertheless, we did observe very slow hydrolysis and condensation of TEOS. An addition of neutral auxiliary templates such as 1.0 g of Brij76 [1.41 mmol, $HO(CH_2CH_2O)_{10}C_{18}H_{35}$], 1.0 g of Pluronic P123 {0.182 mmol, $HO(CH_2CH_2O)_{20}[CH_2CH(CH_3)O]_{70}(CH_2CH_2O)_{20}H$}, and 0.5 g of P123 (0.09 mmol) gave BMS-2, BMS-3, and BMS-4, respectively. In order to evaluate the role of the auxiliary template during the mesophase formation, the amount of CTAOH was fixed at 1.66 mmol. The materials were investigated by using HRSEM with thin metallic coating. The BMS-1 prepared solely from CTAOH exhibited a complex pore structure as represented in Figure 2a. Three-dimensionally interconnected larger mesoscale pores were clearly discerned from the HRSEM image. BMS-2 and BMS-3 also exhibited similar structures as shown in Figure 2. BMS-1 showed a weak, broad diffraction peak at $2\theta = 1.82°$ (d = 4.85 nm) from the XRD diffraction pattern shown in Figure 3. This may indicate a lower degree of ordering of smaller mesopores. However, this weak and broad peak may also reflect the small domain size of the mesostructures. This is supported by TEM images in Figure 6 (domain size ca. 30 nm). Both BMS-2 and BMS-3 did not show any diffraction peaks in the measured 2θ range. BMS-4 prepared by using half the amount of P123 relative to that used for BMS-3 also showed a weak broad peak at $2\theta = 1.64°$ (d = 5.39 nm).

The detailed pore structure was revealed from the Brunauer–Emmett–Teller (BET) isotherm and Barrett–Joyner–Hallenda (BJH) pore-size distribution as depicted in Figures 4 and 5, respectively. Bimodal porosity was unequivocally confirmed from the BJH pore-size distribution curves obtained from N_2 sorption analysis at 77 K. Most of the calcined samples possess smaller mesopores (ca. 3.0 to 3.7 nm) as well as additional larger mesopores ranging from 16 to 35 nm depending on the presence or the amount of neutral auxiliary template. For example, BMS-2 prepared by using a mixture of CTAOH and Brij76 has two distinct

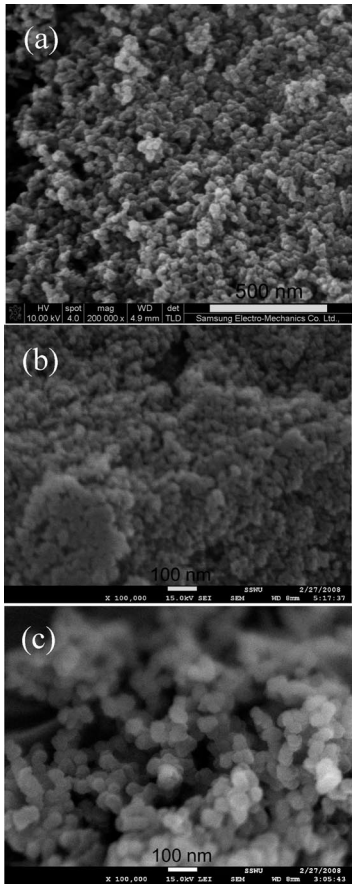

Figure 2. SEM images of the BMS-1 (a), BMS-2 (b), and BMS-3 (c).

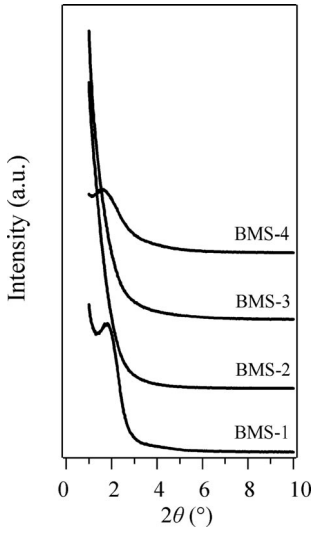

Figure 3. Powder XRD patterns of the BMS samples.

mesopores centered at 3.3 and 16.1 nm, respectively. For BMS-2, the larger mesopore has a narrow pore-size distribution curve, which is indicative of uniformity among the pore-size population. As we reduced the amount of P123 (BMS-4), the second larger mesopore almost disappeared.

Therefore, the cooperative effect of CTAOH and the neutral template is essential to generate well-defined bimodal mesoporosity.

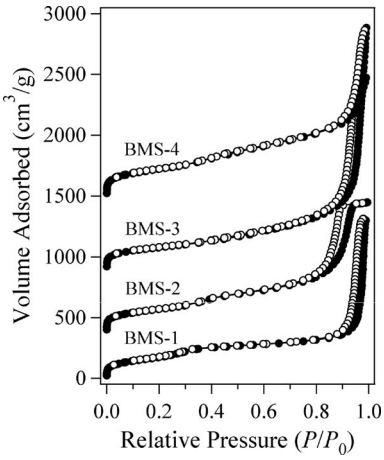

Figure 4. N_2 adsorption/desorption isotherms of the BMS samples at 77 K. Adsorption (●) and desorption (○) branches are indicated.

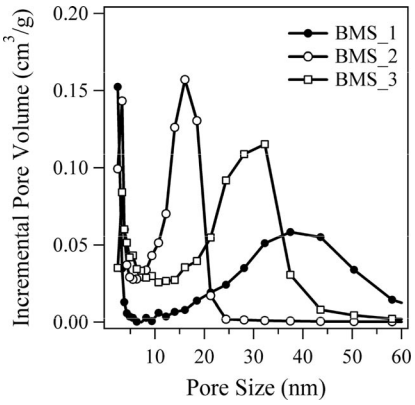

Figure 5. BJH pore-size distribution curves. The pore-size distribution curve for BMS-4 is omitted for clarity.

The BET isotherms display a sharp increase in the adsorbed amount of N_2 between 0.8 and 1.0 P/P_0. The sudden increase in adsorption volume is also indicative of the presence of second larger mesopores.[6] Furthermore, the pattern of the BET isotherm is closely related to those of the typical bimodal nanoporous materials.[7] There is no significant hysteresis between the adsorption and desorption branches. The BMS materials showed high surface areas and pore volumes. For instance, BMS-1 showed BET surface area and pore volume of 688 m^2/g and 2.01 cm^3/g, respectively. The detailed surface area and pore volume data are summarized in Table 1.

Further evidence of the well-defined bimodal porosity was directly obtained from TEM investigation. TEM images are depicted in Figure 6. They show very interesting nanostructures resulting from the unique pore orientation and geometry of the smaller mesopores. BMS-1 and BMS-2 exhibited a fascinating dissimilarity of the pore orientations. The smaller mesopores in BMS-1 are disordered

Table 1. Textural properties of the BMS and BMC materials.

Sample	S_{BET} (m^2/g)	V_p (cm^3/g)	Pore size[a] (nm)	Pore size[b] (nm)
BMS-1	688	2.01	–	37.4
BMS-2	627	1.62	3.3	16.1
BMS-3	634	2.42	3.3	32.3
BMS-4	790	2.10	–	–
BMC-1	961	0.92	3.8	–
BMC-2	1328	2.08	5.5, 9.4	18.5
BMC-3	1069	1.39	3.3	21.3
BMC-4	970	0.85	–	28.1

[a] For the smaller pore. [b] For the larger mesopore.

along the thin silica wall (Figure 6a), whereas the pores in BMS-2 run parallel with respect to the longitudinal axis of the silica wall (Figure 6b). Moreover, BMS-3 showed spherical cage-type mesopores as shown in Figure 6c. These discrepancies of the pore structures are attributed to the different interfacial interactions between CTAOH and the neutral auxiliary templates. Therefore, the auxiliary templates play a significant role in determining the nanostructure of the mesopores. The mesoporous carbonaceous materials were also successfully prepared through a nanocasting process by using the BMS materials as hard templates and furfuryl alcohol as a carbon source followed by carbonization at 1073 K under an atmosphere of N_2. We used 50 vol.-% of furfuryl alcohol relative to the measured pore volumes of the BMS materials to prevent complete infiltration of available pores by the carbon precursors. Pure carbonaceous materials were obtained by HF etching. The oxygen contents of the samples were determined from elemental analysis: BMC-1, 2.6%; BMC-2, 1.9%; BMC-3, 3.2%; and BMC-4, 2.7% (BMC-*n* was obtained from BMS-

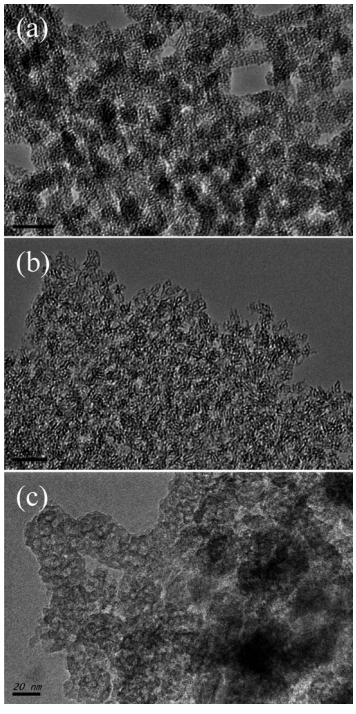

Figure 6. TEM images of BMS-1 (a), BMS-2 (b), and BMS-3 (c). Scale bars: 50 nm for (a) and (b), 20 nm for (c).

n). The SEM and TEM images of the bimodal mesoporous carbon (BMC) materials are shown in Figures 7 and 8, respectively. Although the BMC materials did not show any diffraction peaks between 1 and 10° (data not shown), they showed good mesoporosity (Figure 8). As shown in Figure 7, BMC-2 and BMC-3 possess much thinner carbon walls than those of BMC-1 and BMC-4 owing to the differences in the secondary mesopore dimensions of the silica templates. The three-dimensional pore structures were well preserved during the carbonization and HF etching processes. BMC-2 obtained from siliceous BMS-2 exhibited the highest surface area of 1328 m^2/g with a pore volume of 2.08 cm^3/g (Table 1). The BET isotherms of the all BMC materials showed a typical type IV shape without a significant hysteresis (Figure 9). The BMC materials also exhibited bimodal porosity as shown in Figure 10.

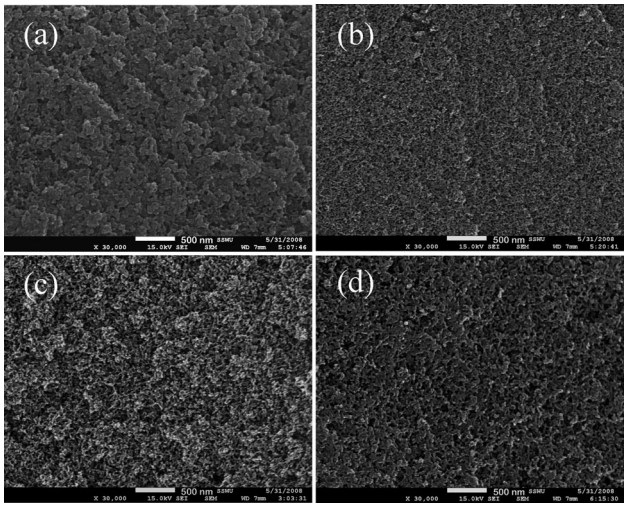

Figure 7. SEM images of BMC-1 (a), BMC-2 (b), BMC-3 (c), and BMS-4 (d). Scale bars = 500 nm.

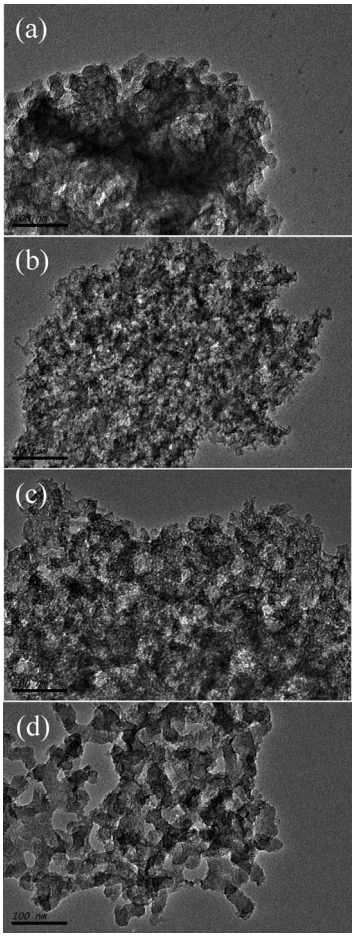

Figure 8. TEM images of BMC-1 (a), BMC-2 (b), BMC-3 (c), and BMC-4 (d). Scale bars = 100 nm. Bimodal nature of the samples is clearly visible.

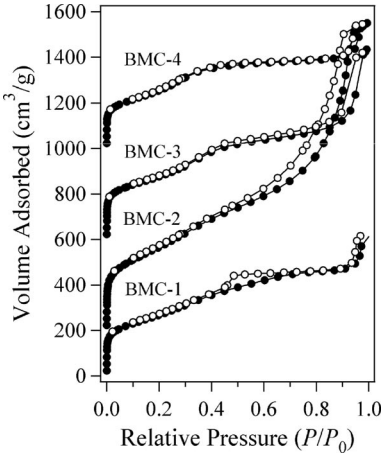

Figure 9. N_2 adsorption/desorption isotherms of the BMC samples at 77 K. Adsorption (●) and desorption (○) branches are indicated.

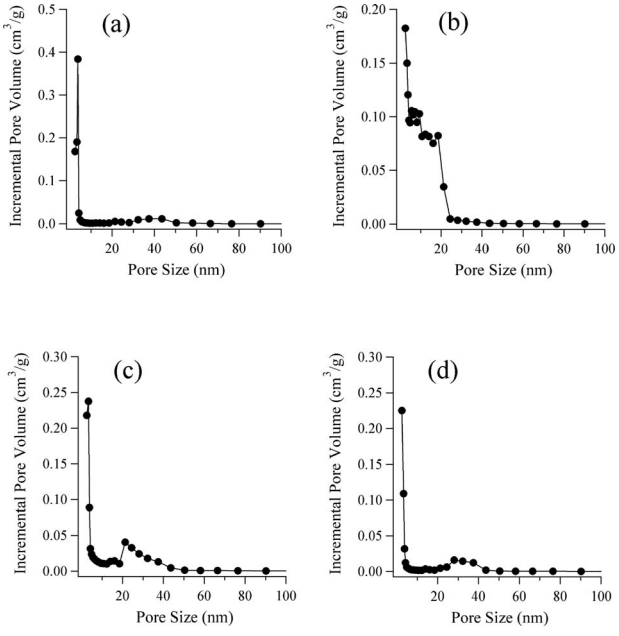

Figure 10. BJH pore-size distribution curves of the BMC materials: BMC-1 (a), BMC-2 (b), BMC-3 (c), and BMC-4 (d).

Hydrogen storage capacities of the BMC materials were studied at 77 K. The hydrogen uptake capacities ranged from 1.11–1.33 wt.-% as shown in Figure 11. The uptake values of the BMC materials are quite comparable to those of other carbon-based adsorbents reported so far.[8] Despite the lower surface area and pore volume of BMC-3 relative to those of BMC-2, BMC-3 exhibited the highest hydrogen uptake of 1.33 wt.-%. In fact, BMC-3 has the narrowest pores (Table 1), while keeping a relatively large pore volume. There are several accounts in the literature linking small pore size of carbons with enhanced hydrogen uptake.[9]

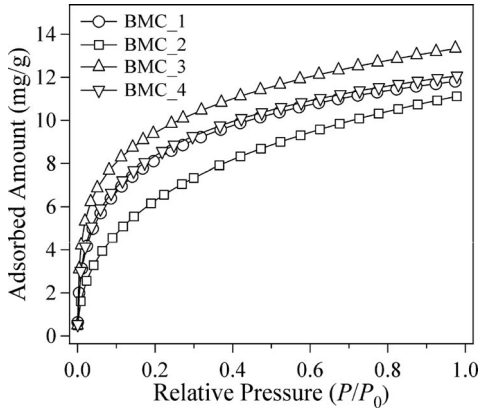

Figure 11. Low-pressure hydrogen adsorption measured at 77 K.

Conclusions

In summary, we successfully prepared a series of siliceous and carbonaceous materials with complex nanostructures through a very simple route. Our approach involving the employment of CTAOH not only as a mesoscale template but also as a hydrolysis/condensation catalyst led us to develop an efficient preparation method of a series of multilength-scale porous materials. By adding a suitable amount of neutral auxiliary templates such as Brij76 or P123, it was possible to finetune the average pore diameter of the larger secondary pores. In addition, the unique role of Brij76 and P123 to alter mesopore nanostructures turned out to be very effective. Bimodal mesoporous carbons with a decent hydrogen sorption ability were also prepared through the nanocasting process by using the bimodal silica mesoporous silicas as hard templates. These nanoporous materials with multilength-scale pores can be used as catalyst supports, adsorbents, biomolecule sequestering agents, and hydrogen storage media.

Experimental Section

Synthesis of the BMS Materials: A homogeneous mixture of CTAOH (10 wt.-% aqueous solution, 5.0 g, 1.66 mmol, TCI) and deionized water (240 g, 13.3 mol) was heated at 353 K under constant stirring for about 1 h (500 rpm). TEOS (4.0 g, 19.2 mmol, Aldrich) was injected rapidly into the mixture. The reaction mixture was stirred at 353 K for 24 h. As-prepared BMS-1 was recovered by hot filtration and washed with a copious amount of water. The isolated solid was dried in air overnight. Template-free BMS-1 was obtained by calcination in air at 823 K for 6 h. BMS-2 was prepared by adding Brij76 (1.0 g, 1.41 mmol, TCI) into the aforementioned reaction mixture. P123 (1.0 g, 0.182 mmol, Aldrich) was added to the reaction mixture for the preparation of BMS-3. Other preparation conditions were identical unless otherwise noted.

Synthesis of the BMC Materials: The preparation of BMC-1 from BMS-1 is described. BMS-1 (0.5 g) was suspended in a solution of *p*-toluenesulfonic acid (*p*TSA; 0.5 M in ethanol, 50 mL). The suspension was gently stirred at room temperature for 5 h. The solid material was retrieved by filtration and dried at 353 K for 2 h. Furfuryl alcohol (1.0 mL) was mixed with *p*TSA-loaded BMS-1. The solids were carbonized at 1073 K under an N_2 flow for 2 h (ramping rate = 2 °C/min). The resulting solids were immersed into an aqueous solution of HF (48 wt.-%, 30 mL) and maintained at room temperature for 12 h. Silica-free BMC-1 was obtained by filtration and washed with a copious amount of water. BMC-1 was further dried at 353 K overnight.

Physical Measurements: TEM images were obtained with a JEOL JEM-2100F operating at 200 kV. The sample suspension in acetone was dropped on the carbon-coated Cu TEM grid and air dried before measurement. FESEM images were obtained with a Jeol JSM-7500F or FEI Nova 200 NanoSEM. Powder XRD spectra were obtained with a Bruker D8 Focus diffractometer (40 kV, 30 mA). The oxygen contents of the carbonaceous samples were analyzed by using a EA1112 (CE Instruments, Italy). The N_2 sorption analysis was performed with a Belsorp-miniII at 77 K (BEL Japan). The samples were dried at 423 K under high vacuum for 2 h. Low-pressure hydrogen adsorption measurements were performed at 77 K with a Belsorp-miniII. The equipment was calibrated by using Cu-BTC (HKUST-1) as a reference material. As-prepared HKUST-1 activated at 393 K under high vacuum for 2 h showed a hydrogen uptake value of 2.23 wt.-% at 77 K and 1 bar. This value agrees well with the reported value (2.27 wt.-%) under the same conditions.[10] All other samples were dried at 423 K for 2 h under high vacuum prior to the measurements.

Acknowledgments

This work was supported by the Gyeonggi Regional Research Center (GRRC) program of Gyeonggi province (PR08013). The authors also thank Mr. K. Kim for technical assistance.

[1] a) M. E. Davis, *Nature* **2002**, *417*, 813–821; b) S. Dai, M. C. Burleigh, Y. Shin, C. C. Morrow, C. E. Barnes, Z. Xue, *Angew. Chem. Int. Ed.* **1999**, *38*, 1235–1239; c) J. Y. Ying, C. P. Mehnert, M. S. Wong, *Angew. Chem. Int. Ed.* **1999**, *38*, 56–77; d) G. J. de A. A. Soler-Illia, C. Sanchez, B. Lebeau, J. Patarin, *Chem. Rev.* **2002**, *102*, 4093–4138; e) Z.-Y. Yuan, B.-L. Su, *J. Mater. Chem.* **2006**, *16*, 663–677.

[2] a) C. T. Kresge, M. E. Leonowicz, W. J. Roth, J. C. Vartuli, J. S. Beck, *Nature* **1992**, *359*, 710–712; b) J. S. Beck, J. C. Vartuli, W. J. Roth, M. E. Leonowicz, C. T. Kresge, K. D. Schmitt, C. T.-W. Chu, D. H. Olson, E. W. Sheppard, S. B. McCullen, J. B. Higgins, J. L. Schlenkert, *J. Am. Chem. Soc.* **1992**, *114*, 10834–10843.

[3] a) S. Yang, X. Zhou, P. Yuan, M. Yu, S. Xie, J. Zou, G. Q. Lu, C. Yu, *Angew. Chem. Int. Ed.* **2007**, *46*, 8579–8582; b) H. Chen, J. He, *Chem. Commun.* **2008**, 4422–4424.

[4] a) S. Huh, J. W. Wiench, J.-C. Yoo, M. Pruski, V. S.-Y. Lin, *Chem. Mater.* **2003**, *15*, 4247–4256; b) S. Huh, J. W. Wiench, B. G. Trewyn, S. Song, M. Pruski, V. S.-Y. Lin, *Chem. Commun.* **2003**, 2364–2365.

[5] a) Q. Cai, Z.-S. Luo, W.-Q. Pang, Y.-W. Fan, X.-H. Chen, F.-Z. Cui, *Chem. Mater.* **2001**, *13*, 258–263; b) J. Lu, E. Choi, F. Tamanoi, J. I. Zink, *Small* **2008**, *4*, 421–426.

[6] H. Yamada, H. Nakamura, F. Nakahara, I. Moriguchi, T. Kudo, *J. Phys. Chem. C* **2007**, *111*, 227–233.

[7] a) A.-H. Lu, W. Schmidt, B. Spliethoff, F. Schüth, *Adv. Mater.* **2003**, *15*, 1602–1606; b) F. Jiao, A. H. Hill, A. Harrison, A. Berko, A. V. Chadwick, P. G. Bruce, *J. Am. Chem. Soc.* **2008**, *130*, 5262–5266.

[8] N. Texier-Mandoki, J. Dentzer, T. Piquero, S. Saadallah, P. David, C. Vix-Guterl, *Carbon* **2004**, *42*, 2744–2747.

[9] a) A. Gigras, S. K. Bhatia, A. V. Anil Kumar, A. L. Myers, *Carbon* **2007**, *45*, 1043–1050; b) A. W. C. van den Berg, C. O. Areán, *Chem. Commun.* **2008**, 668–681; c) Y. Gogotsi, R. K. Dash, G. Yushin, T. Yildirim, G. Laudisio, J. E. Fischer, *J. Am. Chem. Soc.* **2005**, *127*, 16006–16007; d) X. B. Zhao, B. Xiao, A. J. Fletcher, K. M. Thomas, *J. Phys. Chem. B* **2005**, *109*, 8880–8888.

[10] B. Xiao, P. S. Wheatley, X. Zhao, A. J. Fletcher, S. Fox, A. G. Rossi, I. L. Megson, S. Bordiga, L. Regli, K. M. Thomas, R. E. Morris, *J. Am. Chem. Soc.* **2007**, *129*, 1203–1209.

Received: February 16, 2009
Published Online: May 26, 2009

